



# Numerical study on heat transfer enhancement and flow characteristics of double pipe heat exchanger fitted with rectangular cut twisted tape

Ali Barzegar<sup>1</sup> · Dovood Jalali Vahid<sup>1</sup>

Received: 15 December 2018 / Accepted: 27 May 2019 / Published online: 14 June 2019  
© Springer-Verlag GmbH Germany, part of Springer Nature 2019

## Abstract

In the present study, the heat transfer, friction factor and thermal performance factor of rectangular cut twisted tape (RCT) that are inserted in inner tube side of a double pipe heat exchanger (DPHE) are numerically examined. The obtained results have been compared with the performance of heat exchangers, which are equipped/unequipped by typical twisted tape (TT). The RCTs have constant twist ratio ( $Y = 3.0$ ) and are used in different cut depth ratios ( $DR = 0.15, 0.24$  and  $0.33$ ) and cut width ratios ( $WR = 0.15, 0.24$  and  $0.33$ ). The investigated Reynolds number range is from 6000 to 18,000 and the working fluid is considered to be water. Hot water with a variable mass flow rate is flowing through the inner pipe but cold water has counter flow through annulus side with constant mass flow rate. For the selection of the turbulence model and validation, the obtained numerical results for plain double pipe heat exchanger (P-DPHE) and heat exchanger with TT are compared with empirical correlations. Then the more accurate model was used to simulate the RCTs cases. Comparing the simulation results for RCTs and TT, it was determined that Nusselt number, friction factor and thermal performance factor will have higher value when using RCTs. This behavior is directly and inversely proportional to the DR and WR respectively. In this study, the highest thermal performance factor is about 1.46 which is obtained for RCTs in  $DR = 0.33$  and  $WR = 0.15$  conditions. In addition, new empirical correlations have been offered for calculating a Nusselt number and friction factor for inserted rectangular cut twisted tape in a tube.

## Nomenclature

$C_1, C_2, C_{1\varepsilon}, C_{2\varepsilon}, C_\mu$	Model constant	$G_\omega$	Generation of specific dissipation rate
$C_p$	Specific heat capacity at constant pressure, $J/kg K$	$h$	Heat transfer coefficient, $W/(m^2K)$
$CD_{\kappa\omega}$	Cross-diffusion term, $Kg/m S^2$	$k$	Thermal conductivity, $W/(mK)$
$d$	Rectangular cut depth, $m$	$L$	Length of tube, $m$
$D$	Diameter of tube, $m$	$\dot{m}$	Mass flow rate, $kg/s$
$D_h$	Hydraulic diameter, $m$	$Nu$	Nusselt number
$E$	Energy, $J$	$p$	Pitch length based on $180^\circ$ , $m$
$f$	Friction factor	$P$	Pressure, $Pa$
$F_1, F_2$	Blending function	$\Delta P$	Pressure drop, $Pa$
$G_\kappa$	Generation of turbulence kinetic energy due to the mean velocity gradients	$Pr$	Prandtl number
		$Q$	Heat transfer rate, $W$
		$Re$	Reynolds number
		$R_\varepsilon$	Term relating to the mean strain and turbulence quantities
		$S$	Invariant measure of the strain rate, $1/s$
		$t$	Time, $s$
		$T$	Temperature, $^\circ C$
		$u$	Average velocity, $m/s$
		$w$	Rectangular cut width, $m$
		$W$	Width of twisted tape, $m$
		$x$	Axial coordinate, $m$

✉ Ali Barzegar  
a\_barzegar@sut.ac.ir

Dovood Jalali Vahid  
davoodjalali@sut.ac.ir

<sup>1</sup> Department of Mechanical Engineering, Sahand University of Technology, Tabriz 51335-1996, Iran

$y$	Shortest distance to the near wall, $m$
$Y$	Twist ratio, $(p/W)$

### Greek symbols

$\alpha_\varepsilon$	Inverse Prandtl numbers for $\varepsilon$
$\alpha_\kappa$	Inverse Prandtl numbers for $k$
$\beta_1, \beta_2, \beta^*$	Turbulent modeling constant
$\gamma$	Turbulent modeling constant
$\delta_{ij}$	Kronecker delta
$\delta$	Thickness of tape, $m$
$\varepsilon$	Turbulent dissipation rate, $m^2/s^3$
$\kappa$	Turbulent kinetic energy, $m^2/s^2$
$\mu$	Dynamic viscosity, $kg/ms$
$\nu$	Kinematic eddy viscosity, $m^2/s$
$\rho$	Density, $kg/m^3$
$\sigma_\varepsilon$	Turbulent Prandtl numbers for $\varepsilon$
$\sigma_\kappa$	Turbulent Prandtl numbers for $k$
$\sigma_\omega$	Turbulent Prandtl numbers for $\omega$
$\tau_{ij}$	Turbulent Reynolds stress tensor $kg/ms^2$
$\omega$	Specific dissipation rate, $1/K$

### Subscripts

$a$	Annulus side
$c$	Cold
$eff$	Effective
$h$	Hot
$i$	Inner tube side
$in$	Inlet
$out$	Outlet
$p$	Plain tube
$t$	Turbulent

### Abbreviations

<i>DPHE</i>	Double pipe heat exchanger
<i>DR</i>	Rectangular cut depth ratio, $(d/W)$
<i>P-DPHE</i>	Plain double pipe heat exchanger
<i>RANS</i>	Reynolds-averaged Navier-Stokes (equations)
<i>RCT</i>	Rectangular cut twisted tape
<i>RNG</i>	Re-Normalization Group
<i>SST</i>	Shear stress transport
<i>TPF</i>	Thermal performance factor
<i>TT</i>	Typical twisted tape
<i>WR</i>	Rectangular cut width ratio, $(w/W)$

## 1 Introduction

In recent years, different methods have been developed for heat transfer enhancement in heat exchangers, which will lead to a reduction in the cost and size of them. Two major methods for increasing heat transfer rate are active and passive methods. In the active method, external forces such as magnetic field or surface vibration are used to disrupt the boundary layer and increase turbulence to achieve higher heat transfer rate, while in the passive method an external device such as coil wires and twisted-tapes are used inside the tube. These devices create a

turbulent flow, which increases the heat transfer rate and due to their lower cost, they are usually paid more attention [1]. Twisted tapes can easily be used inside the heat exchangers. In addition, maintenance of these insertions is very easy. With the use of twisted tape, a turbulent flow is created inside the tube and the turbulence intensity increases, which is an important factor in increasing the amount of heat transfer rate [2–5]. However, it should be noted that the use of twisted tapes would also increase the undesirable pressure drop in the tube [6–10]. Different numerical and experimental studies have been conducted for investigating the modified twisted tapes insertion in the tube and its effect on the heat transfer rate. Skullong et al. [11] studied the impact of the curved-winglet tapes in the heat exchanger tube. They had chosen three relative winglet heights (0.1, 0.2 and 0.3) and winglet pitches (0.5, 1.0 and 2.0). The results showed that the maximum thermal enhancement factor is about 1.62 at winglet height and winglet pitch of 0.1 and 1.0 respectively. Zhang et al. [12] numerically investigated heat transfer and fluid flow characteristics of a tube equipped with helical screw-tape without core-rod inserts. For these tapes, they considered four different widths with four different inlet volume-flow rates. The results show that heat transfer and friction factor for helical screw-tape with all widths are higher than a plain tube. He et al. [13] discovered experimentally the effect of cross hollow twisted tape in a tube. The results show that when hollow width increases, the Nusselt number and the friction factor first decrease but then increase and the performance evaluation criterion varies from 0.87 to 0.98. Nana et al. [14] presented experimental results for tube fitted with perforated helical twisted tapes and the parameters examined are the perforated helical twisted tapes diameter ratios and perforation pitch ratios. The results indicate that with a decrease in diameter ratios and an increase in perforation pitch ratios, the heat transfer, friction loss, and thermal performance factor increase. In their study, the maximum performance factor was 1.28. Oni et al. [15] numerically studied the heat transfer and flow characteristics of water in a circular tube with the insertion of different modified twisted tapes. According to the results, the tube with alternate-axis triangular cut twisted tape and typical twisted tape have the highest and lowest value for thermal performance factor respectively. In a number of studies, twisted tapes with different perforated geometries have been investigated which were conducted numerically by Mashoofi et al. [16] and Saysroy and Eiamsa-ard [17] and experimentally by Suri et al. [18] and Thianpong et al. [19, 20]. The results show that depending on the perforated geometry, the Nusselt number and thermal performance factor of modified tapes can be more or less than typical twisted tape. Man et al. [21] experimentally used different twisted tapes inside the inner tube of double tube heat exchanger and investigated the Nusselt number and the friction factor in these tubes. The used twisted tapes were clockwise and counterclockwise twisted tape (ACCT tape) and typical twisted tape. The results indicated that the ACCT

tapes show better performance than the typically twisted tapes for which the best result has appeared with the full-length of ACCT tape. In other experimental studies, Ferroni et al. [22] and Eiamsa-ard [23] investigated pressure drop on a horizontal round tube in which it was equipped with separated, multiple, short-length twisted tape. The results show that the separated short-length twisted tapes have lower pressure drops in comparison to the full-length tapes. Recently, Zheng et al. [24] conducted a numerical study using dimpled twisted tapes in circular tubes. They investigated the effects of dimple and protrusion sides on heat transfer enhancement and flow characteristic of tubes. Their results indicate that the presence of both dimples and protrusions sides increase the heat transfer enhancement. In the meanwhile, dimples sides offer better results in comparison with protrusions sides. Eiamsa-ard et al. experimentally studied various modified twisted tapes including: twin-counter/co-twisted tapes [25], twisted tapes consisting of center wings and alternate-axes [26], uniform/non-uniform twisted-tapes with alternate axes [27], alternate clockwise and counter-clockwise twisted-tape [28], peripherally-cut twisted tape [29] and delta-winglet twisted tape [30]. Their results in various studies show that the use of modified twisted tapes has a higher heat transfer rate and thermal performance factor in comparison with typical twisted tape. In a numerical study by El Maakoul et al. [31], the thermal-hydraulic performance of a double pipe heat exchanger in which helical baffles was used in the annulus side, is investigated. The simulation results show that the thermal performance and pressure drop of these pipes are increased in comparison with the simple double pipe exchangers and this increase is a function of baffle spacing and Reynolds number. Guo et al. [32] presented a numerical study on the heat transfer enhancement and flow characteristics of the tubes equipped with helical screw-tape inserts. The obtained results reveal that the heat transfer rate in the helical inserts with right and left twists is higher than helical inserts with uniformly right twists. Murugesan et al. [33] reported the experimental data for V-cut twisted tape insertion into the inner pipe of double pipe heat exchangers. Their studied parameters are twisted ratio, V-cut depth ratio, and width ratio. The results show that for V-cut twisted tapes, by increasing cut depth ratios and decreasing cut width ratios or twist ratios, the Nusselt number, friction factor and thermal performance factor are increased. In an experimental study, Seemawute and Eiamsa-ard [34] investigated the peripherally-cut twisted tape in the tube. The obtained results show that the use of peripherally-cut twisted tape results in a higher heat transfer rate than a typical twisted tape and empty tube. The highest thermal performance factor obtained in this study is equal to 1.25.

By reviewing previous studies, it can be concluded that the use of a modified twisted tape with proper geometry has a significant effect on heat transfer and flow characteristics. In addition, by applying some cuts with specific shapes along the edge of tapes, the heat transfer rate can be increased, in

comparison with typical twisted tape [5, 29, 33, 35, 36]. In the present article, the effects of rectangular cut twisted tape (RCT) insertion into the inner pipe of double pipe heat exchanger is investigated numerically. The cuts are created along the two edges of the tape and the study parameters are cut depth ratio that is defined as the ratio of rectangular cut depth to the tape maximum width ( $DR = d/W$ ) and cut width ratio that is defined as the ratio of rectangular cut width to the tape maximum width ( $WR = w/W$ ). These parameters are evaluated for three values ( $DR = 0.15, 0.24$  and  $0.33$ ) and ( $WR = 0.15, 0.24$  and  $0.33$ ) at constant twist ratio ( $Y = p/W = 3.0$ ). The working fluid is water and the Reynolds number range is between 6000 and 18,000. Moreover, by studying double pipe heat exchanger with/without typical twisted tape (TT) in the same conditions and comparing their results with the RCTs, the effect of the modified twisted tape parameters on the heat transfer rate (Nu), friction factor (f) and thermal performance factor (TPF) is characterized.

## 2 Physical model

### 2.1 Double pipe heat exchanger

Numerical simulation were carried out in a double pipe heat exchanger (DPHE). The geometrical specifications and also other details of simulated heat exchanger are illustrated in Fig. 1 and Table 1.

### 2.2 Twisted tapes

The twisted tapes (RCT or TT) are used in the total length of the inner tube and their material is considered to be stainless steel. The geometrical specifications of all inserted tapes which are used in this study were shown in Table 2 and illustrated schematically in Fig. 2.

## 3 Numerical simulations

### 3.1 Governing equations

For the simplicity of calculation, some assumptions are considered for the working fluid. Water is assumed to be Newtonian, incompressible and flows in steady state condition. The effect of

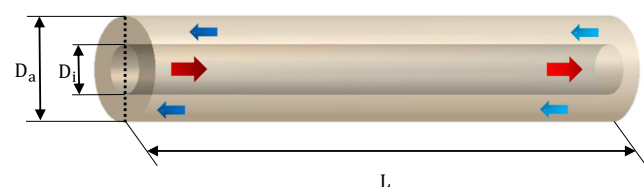


**Fig. 1** Schematic diagram of counter flow double pipe heat exchanger. **a** Inner tube side equipped with rectangular cut twisted tape (RCT). **b** Inner tube side equipped with typical twisted tape (TT)

**Table 1** Geometry details of double pipe heat exchanger

Section	Length (L)	Diameter	Thickness	Material	Flow fluid
Inner tube	1000 mm	$D_i = 14$ mm	0.5 mm	Copper	Hot Water
Annulus	1000 mm	$D_a = 32$ mm	1.0 mm	Copper	Cold water

gravity can be neglected and the chemical reaction and thermal radiation are ignored. The Navier–Stokes equations (or RANS equations) in steady form are used to govern the heat transfer which can be written in the form of a tensor as follows [37]:

Continuity equation:

$$\frac{\partial}{\partial x_i}(\rho u_i) = 0 \tag{1}$$

Momentum equation:

$$\frac{\partial(\rho u_i u_j)}{\partial x_j} = -\frac{\partial P}{\partial x_i} + \frac{\partial}{\partial x_i} \left[ \mu \left( \frac{\partial u_i}{\partial x_j} + \frac{\partial u_j}{\partial x_i} - \frac{2}{3} \delta_{ij} \frac{\partial u_k}{\partial x_k} \right) \right] + \frac{\partial}{\partial x_j} (-\rho \overline{u_i u_j}) \tag{2}$$

Energy equation:

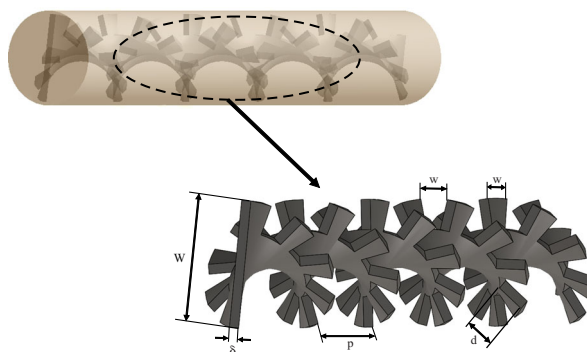
$$\frac{\partial}{\partial x_i} [u_i(\rho E + P)] = \frac{\partial}{\partial x_j} \left( k_{eff} \frac{\partial T}{\partial x_j} \right), \quad E = h - \frac{P}{\rho} + \frac{u^2}{2} \tag{3}$$

Where  $\mu$  is the dynamic viscosity of working fluid,  $\rho$  is fluid density and  $k_{eff}$  is effective thermal conductivity which is expressed as:

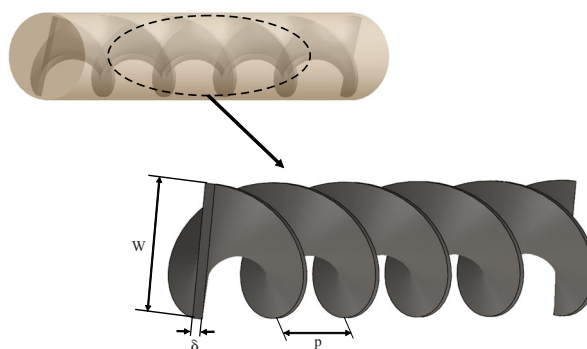
$$k_{eff} = k + C_p \frac{\mu_t}{Pr_t} \tag{4}$$

### 3.2 Turbulence Modelling

By examining previous studies, it is clear that different turbulence models have been used to simulate a turbulent flow



(a) Inner tube side equipped with rectangular cut twisted tape (RCT)



(b) Inner tube side equipped with typical twisted tape (TT)

**Fig. 2** The geometrical configurations of inner tube side equipped with different types of twisted tapes

inside the tube such as RNG  $\kappa - \epsilon$  [18], realizable  $\kappa - \epsilon$  [31] and SST  $\kappa - \omega$  [24]. In the present article, these models are evaluated for heat exchanger with/without TT and the obtained results are compared with empirical correlations in order to choose the most precise model to simulate the cases in which rectangular cut twisted tapes are used.

**Table 2** Geometry details of used twisted tapes

Twisted tape	Length	Rectangular cut width w	Maximum width W	Thickness $\delta$	Twist ratio $y = p/w$	Cut depth ratio $DR = d/W$	Cut width ratio $WR = w/W$
TT	1000 mm	–	13 mm	1.0 mm	3.0	–	–
RCT	1000 mm	1.95 mm	13 mm	1.0 mm	3.0	0.15	0.15
RCT	1000 mm	3.12 mm	13 mm	1.0 mm	3.0	0.15	0.24
RCT	1000 mm	4.29 mm	13 mm	1.0 mm	3.0	0.15	0.33
RCT	1000 mm	1.95 mm	13 mm	1.0 mm	3.0	0.24	0.15
RCT	1000 mm	3.12 mm	13 mm	1.0 mm	3.0	0.24	0.24
RCT	1000 mm	4.29 mm	13 mm	1.0 mm	3.0	0.24	0.33
RCT	1000 mm	1.95 mm	13 mm	1.0 mm	3.0	0.33	0.15
RCT	1000 mm	3.12 mm	13 mm	1.0 mm	3.0	0.33	0.24
RCT	1000 mm	4.29 mm	13 mm	1.0 mm	3.0	0.33	0.33

### 3.2.1 RNG $\kappa - \varepsilon$ model

The RNG  $\kappa - \varepsilon$  model is a two-equation model that is derived from the Navier-Stokes equations. This is done by a mathematical technique called Re-Normalization Group (RNG) [39]. The results of the analytic derivation will result in constants and additional terms in the transport equations for  $\kappa$  and  $\varepsilon$  which are different from the standard model.  $\kappa$  and  $\varepsilon$  show the kinetic energy of turbulence and the energy dissipation rate, respectively. These equations are [37]:

$$\frac{\partial}{\partial t}(\rho\kappa) + \frac{\partial}{\partial x_i}(\rho\kappa u_i) = \frac{\partial}{\partial x_j} \left[ \alpha_\kappa \mu_{eff} \frac{\partial \kappa}{\partial x_j} \right] + G_\kappa - \rho\varepsilon \tag{5}$$

$$\frac{\partial}{\partial t}(\rho\varepsilon) + \frac{\partial}{\partial x_i}(\rho\varepsilon u_i) = \frac{\partial}{\partial x_j} \left[ \alpha_\varepsilon \mu_{eff} \frac{\partial \varepsilon}{\partial x_j} \right] + C_{1\varepsilon} \frac{\varepsilon}{\kappa} G_\kappa - C_{2\varepsilon} \rho \frac{\varepsilon^2}{\kappa} - R_\varepsilon \tag{6}$$

In these equations,  $G_\kappa$  represents the generation of turbulence kinetic energy due to the mean velocity gradients, and the quantities  $\alpha_\kappa = 0.7194$ ,  $\alpha_\varepsilon = 0.7194$ ,  $C_{1\varepsilon} = 1.42$ ,  $C_{2\varepsilon} = 1.68$ , and  $C_\mu = 0.0845$  are the model constants.  $\mu_{eff}$  is the effective dynamic viscosity and  $\mu_t$  is turbulent viscosity term defined as below:

$$\mu_{eff} = \mu + \mu_t \tag{7}$$

$$\mu_t = \rho C_\mu \frac{\kappa^2}{\varepsilon} \tag{8}$$

### 3.2.2 Realizable $\kappa - \varepsilon$ model

Another two-equation model is realizable  $\kappa - \varepsilon$  [38], which has an alternative formula for turbulent viscosity, and modified equation for the dissipation rate ( $\varepsilon$ ). These equations are [37]:

$$\frac{\partial}{\partial t}(\rho\kappa) + \frac{\partial}{\partial x_i}(\rho\kappa u_i) = \frac{\partial}{\partial x_i} \left[ \left( \mu + \frac{\mu_t}{\sigma_\kappa} \right) \frac{\partial \kappa}{\partial x_i} \right] + G_\kappa - \rho\varepsilon \tag{9}$$

$$\frac{\partial}{\partial t}(\rho\varepsilon) + \frac{\partial}{\partial x_i}(\rho\varepsilon u_i) = \frac{\partial}{\partial x_i} \left[ \left( \mu + \frac{\mu_t}{\sigma_\varepsilon} \right) \frac{\partial \varepsilon}{\partial x_i} \right] + C_1 G_\kappa \varepsilon - \rho C_2 \frac{\varepsilon^2}{\kappa + \sqrt{\nu\varepsilon}} \tag{10}$$

In these equations the empirical constants are:

$$C_1 = \max[0.43, \mu/(\mu_t + 5)]; C_2 = 1.9; \sigma_\kappa = 1.0; \sigma_\varepsilon = 1.2$$

### 3.2.3 SST $\kappa - \omega$ model

Menter’s  $\kappa - \omega$  shear stress transport (SST) model [39], is a two-equation eddy-viscosity model in which one of the equations is for  $\kappa$  and the other is for  $\omega$  which expresses the turbulent kinetic energy and specific turbulent dissipation rate respectively. The equations are given as below [37]:

$$\frac{\partial(\rho\kappa)}{\partial t} = \bar{\tau}_{ij} \frac{\partial \bar{u}_i}{\partial x_j} - \beta^* \rho \omega \kappa + \frac{\partial}{\partial x_j} \left[ (\mu + \sigma_\kappa \mu_t) \frac{\partial \kappa}{\partial x_j} \right] \tag{11}$$

$$\frac{\partial(\rho\omega)}{\partial t} = \frac{\gamma}{\nu_t} \bar{\tau}_{ij} \frac{\partial \bar{u}_i}{\partial x_j} - \beta \rho \omega^2 + \frac{\partial}{\partial x_j} \left[ (\mu + \sigma_\omega \mu_t) \frac{\partial \omega}{\partial x_j} \right] + 2\rho(1-F_1)\sigma_{\omega 2} \frac{1}{\omega} \frac{\partial \kappa}{\partial x_j} \frac{\partial \omega}{\partial x_j} \tag{12}$$

where the kinematic eddy viscosity is given by

$$\nu_t = \frac{\alpha_1 \kappa}{\max(\alpha_1 \omega, SF_2)} \tag{13}$$

The shear stress is given by

$$\bar{\tau}_{ij} = \mu_t \left( \frac{\partial \bar{u}_i}{\partial x_j} + \frac{\partial \bar{u}_j}{\partial x_i} - \frac{2}{3} \frac{\partial \bar{u}_k}{\partial x_k} \delta_{ij} \right) - \frac{2}{3} \rho \kappa \delta_{ij} \tag{14}$$

The other relations are listed as follows:

$$F_1 = \tanh \left\{ \left\{ \min \left[ \max \left( \frac{\sqrt{\kappa}}{\beta^* \omega y}, \frac{500\nu}{y^2 \omega} \right), \frac{4\sigma_{\omega 2} \kappa}{CD_{\kappa\omega} y^2} \right] \right\}^4 \right\} \tag{15}$$

Where,

$$CD_{\kappa\omega} = \max \left( 2\rho\sigma_{\omega 2} \frac{1}{\omega} \frac{\partial \kappa}{\partial x_j} \frac{\partial \omega}{\partial x_j}, 10^{-10} \right) \tag{16}$$

$$F_2 = \tanh \left\{ \left[ \max \left( \frac{2\sqrt{\kappa}}{\beta^* \omega y}, \frac{500\nu}{y^2 \omega} \right) \right]^2 \right\} \tag{17}$$

Different constants for the SST model are:

$$\beta_1 = \frac{3}{40}, \beta_2 = 0.0828, \beta^* = \frac{9}{100}, \sigma_{\kappa 1} = 0.85, \sigma_{\kappa 1} = 1, \sigma_{\omega 1} = 0.5, \sigma_{\omega 2} = 0.856, \gamma_1 = 0.5532, \gamma_2 = 0.4404.$$

### 3.3 Numerical method and boundary conditions

The finite volume method is used to solve the governing equations of the problem and a SIMPLE (Semi-Implicit Method for Pressure-Linked Equations) algorithm was adopted for coupling speed and pressure. The power-law scheme was applied for the momentum and the second order upwind method was used for energy, turbulence kinetic energy, and turbulence dissipation rate. The convergence criterion was considered to be  $10^{-8}$  for energy but for continuity and velocity components it was determined to be  $10^{-7}$ .

The inlet and outlet boundary conditions for both of inner tube and annulus side was set as the velocity-inlet and the pressure-outlet respectively. Surfaces of solid walls and twisted tapes are subjected to no-slip and no penetration condition. For the annulus side wall, the thermal boundary condition is considered to be insulation and was set to have zero heat flux.

For the common walls between the cold and hot fluids coupling heat transfer was considered as the boundary condition [37]. The cold water and hot water inlet temperature are kept constant and equal to  $15^\circ\text{C}$  and  $50^\circ\text{C}$  respectively. The Reynolds number range for hot fluid is  $6000 < Re < 18000$  but mass flow rate for the cold fluid is kept constant.

### 3.4 Grid independent analysis

In this study, the computational domains were defined as two parts: inner tube and annulus side. For the inner tube side, unstructured mesh with a mix of tetrahedral and wedge (for inflation layer) elements was used. For the annulus side structured mesh with hexagonal elements (Fig. 3) was used. For precise investigation of the formed thermal boundary layer and to resolve the swirling flow, fine grids were utilized near the walls and in the vicinity of the twisted tape surfaces. On the other hand, to reduce the calculation time, coarse grids were used for the other regions. In order to verify the

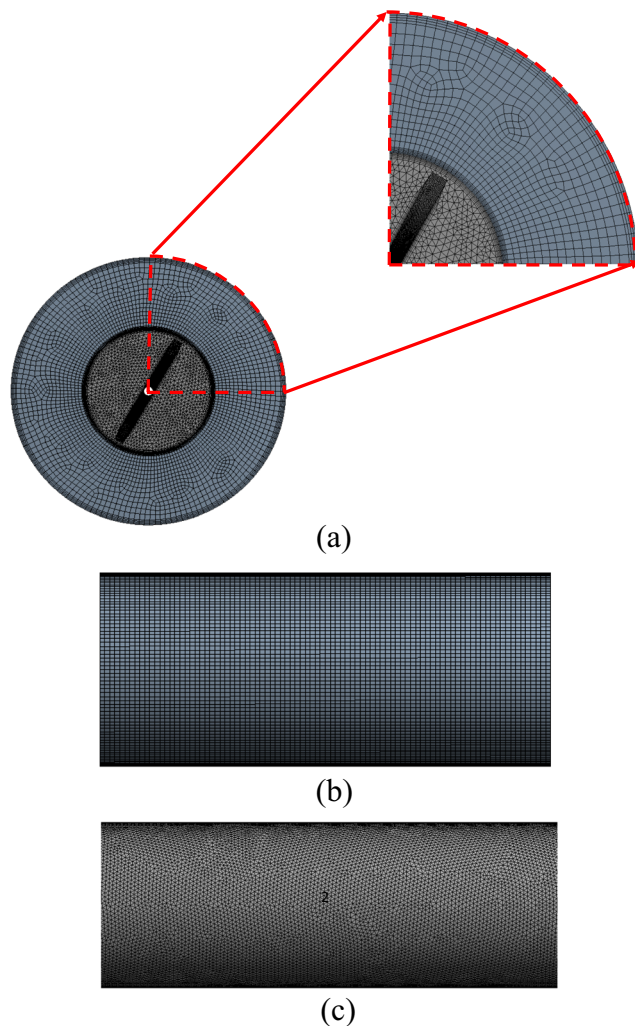


**Fig. 3** The mesh generation in **a** cross section **b** annulus side outer wall **c** common wall between annulus side and inner tube side

independence of simulation results from the grid number, the case of double pipe heat exchanger (DPHE) which is fitted with typical twisted tape (TT) at  $Re = 16,000$  was chosen for an equilibrium between the computation accuracy and grid number. Four different grid numbers:  $\sim 4.58$  million,  $\sim 5.86$  million,  $\sim 7.74$  million and  $\sim 9.32$  million are comparatively evaluated which are shown in Fig. 4. By exploring the data, it is determined that when  $\sim 7.74$  million grid number is used, the differences of  $Nu$  and  $f$  are  $0.65\%$  and  $0.73\%$  in comparison with  $\sim 9.32$  million grid number, respectively. Therefore,  $\sim 7.74$  million grid number is appropriate and provides accurate results. This grid number can be considered as the reference mesh size for other simulation cases. In Table 3, the grid numbers for different simulations have been reported.

### 3.5 Data reduction

The heat transfer rate from the hot water through the inner tube can be obtained as follows:

$$Q_h = \dot{m}_h C_{p,h} (T_{h,in} - T_{h,out}) \quad (18)$$

In addition, the heat transfer rate to the cold water in the annulus side can be calculated from:

$$Q_c = \dot{m}_c C_{p,c} (T_{c,in} - T_{c,out}) \quad (19)$$

Where  $\dot{m}$  is the water mass flow rate,  $C_p$  is the specific heat and  $T$  is the temperature. The subscripts  $h$  and  $c$  refer to hot and cold water respectively.

The average Nusselt number ( $Nu$ ) for the inner tube side is:

$$Nu = h_i D_h / k_i \quad (20)$$

Where  $h_i$  is the heat transfer coefficient,  $D_h$  is equivalent hydraulic diameter and  $k_i$  is thermal conductivity in the inner tube side.

The Reynolds number for the inner tube is given by:

$$Re = \rho_i u_i D_h / \mu_i \quad (21)$$

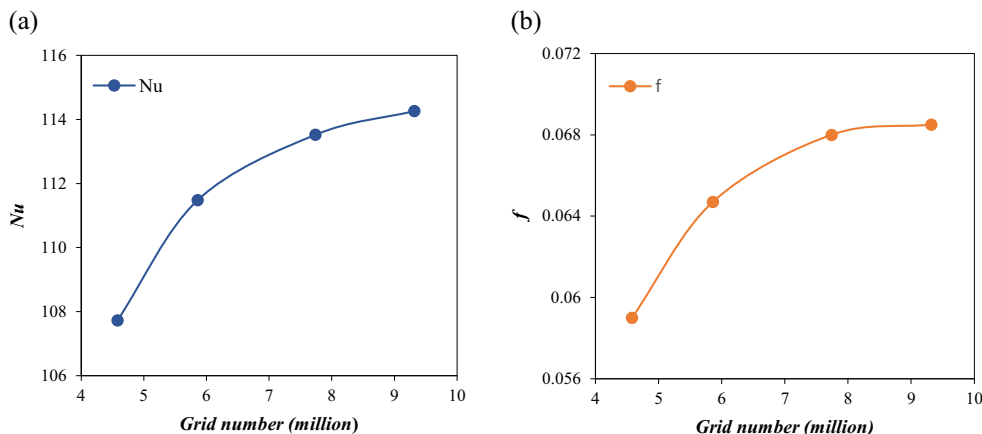
Where  $\rho_i$ ,  $u_i$  and  $\mu_i$  are the density, velocity and dynamic viscosity of the inner tube side, respectively. In addition, the friction factor is calculated from the following equation:

$$f = \frac{\Delta P}{\left(\frac{L}{D_h}\right) \left(\rho_i \frac{u_i^2}{2}\right)} \quad (22)$$

Where  $\Delta P$  is the pressure drop along the tube.

The thermo-physical properties of water can be obtained from the regression equations in Table 4, which must be calculated at the average temperature of the inlet and outlet for each side of the double pipe heat exchanger [40, 41].

**Fig. 4** Grid independence study for **a** Nu and **b** f



### 3.6 Turbulence model selection and results validation

In order to select the appropriate turbulence model from amongst RNG  $\kappa - \epsilon$ , realizable  $\kappa - \epsilon$ , and SST  $\kappa - \omega$  models for the simulation of RCTs cases and to validate the numerical results as well, the double pipe heat exchanger with/without TT was considered for this test. The average Nusselt number (Nu) and friction factor (f) obtained from results were compared with existing empirical correlations. For the plain tubes, the average Nusselt number and the friction factor was calculated by using Gnielinski [42] and Blasius [43] correlations respectively. The Gnielinski correlation is defined as [42]:

$$Nu = \frac{\left(\frac{f}{8}\right)(Re-1000)Pr}{1 + 12.7\left(\frac{f}{8}\right)^{1/2}(Pr^{2/3}-1)} \quad 3000 < Re < 500,000 \tag{23}$$

Moreover, the Blasius correlation is expressed as below [43]:

$$f = 0.316Re^{-1/4} \quad Re \leq 20,000 \tag{24}$$

The obtained simulation results from different turbulence models were compared with the mentioned empirical

correlations (Fig. 5a-b). It is observed that the maximum difference of Gnielinski correlations with any one of the RNG  $\kappa - \epsilon$ , realizable  $\kappa - \epsilon$ , and SST  $\kappa - \omega$  turbulence models is about 8.35%, 6.14% and 9.75% and with Blasius correlation is about 7.53%, 5.84%, and 8.72% respectively. As a result, it can be concluded that the realizable  $\kappa - \epsilon$  turbulence model provides more precise results for the P-DPHE in comparison with other turbulence models.

For heat exchanger with typical twisted tape, the results for the Nusselt number and the friction factor are compared with the suggested correlations by Manglik and Bergles [44]. The correlations they provided are as follows:

For Nusselt number [44]:

$$Nu = 0.023Re^{0.8}Pr^{0.4}\left(1 + 0.769/y\right)\left(\frac{\pi}{\pi-4\delta/D}\right)^{0.8}\left(\frac{\pi+2-2\delta/D}{\pi-4\delta/D}\right)^{0.2} \varnothing \tag{25}$$

Where:

$$\varnothing = (\mu_b/\mu_s)^{0.18} = (T_b/T_s)^{0.45} \tag{26}$$

And for friction factor [44]:

$$f = 0.0791Re^{-0.25}\left(1 + 2.06\left(1 + (2y/\pi)^2\right)^{-0.74}\right)\left(\frac{\pi}{\pi-4\delta/D}\right)^{1.75}\left(\frac{\pi+2-2\delta/D}{\pi-4\delta/D}\right)^{1.25} \tag{27}$$

By examining the simulation results obtained from different turbulence models and comparing them with empirical correlations in Fig. 5c-d, it is observed that the maximum difference of the RNG  $\kappa - \epsilon$ , realizable  $\kappa - \epsilon$ , and SST  $\kappa - \omega$  turbulence models for the Nusselt number is about 9.27%, 7.31% and 11.42% and for the friction factor is about 8.36%, 6.48% and 10.24% respectively. Therefore, it can be said that the realizable  $\kappa - \epsilon$  turbulence model provides more precise results.

By summarizing the results for the P-DPHE and DPHE with TT, it was found that the realizable  $\kappa - \epsilon$  model has more accurate results in comparison with other models. Therefore, this model is used for the simulation of heat exchanger with the RCTs cases.

**Table 3** Summary of total grid number for different study cases

Case study	Grid number
P-DPHE	1,129,752
TT	7,741,249
RCT (DR = 0.15 and WR = 0.15)	8,392,774
RCT (DR = 0.15 and WR = 0.24)	8,386,844
RCT (DR = 0.15 and WR = 0.33)	8,392,868
RCT (DR = 0.24 and WR = 0.15)	8,459,179
RCT (DR = 0.24 and WR = 0.24)	8,447,033
RCT (DR = 0.24 and WR = 0.33)	8,447,530
RCT (DR = 0.33 and WR = 0.15)	8,565,895
RCT (DR = 0.33 and WR = 0.24)	8,515,373
RCT (DR = 0.33 and WR = 0.33)	8,515,777

**Table 4** Estimation of water properties by Regression equations

Properties	Regression equation
Density [40]	$\rho = 1000 \times \left[ 1.0 - \frac{(T-4.0)^2}{119000 + 1365 \times T - 4 \times (T)^2} \right]$
Viscosity [41]	$\mu = 0.00169 - 4.2526e - 5 \times T + 4.925e - 7 \times (T)^2 - 2.099350e - 9 \times (T)^3$
Thermal conductivity [41]	$k = 0.5611 + 0.00193 \times T - 2.60152749e - 6 \times (T)^2 - 6.08803e - 8 \times (T)^3$
Specific heat [41]	$C_p = 4217.629 - 3.20888 \times T + 0.09503 \times (T)^2 - 0.00132 \times (T)^3 + 9.415e - 6 \times (T)^4 - 2.5479e - 8 \times (T)^5$

### 4 Numerical results and discussion

In this section, the effect of insertion rectangular cut twisted tapes (RCT) on temperature field, velocity distributions, turbulent kinetic energy, Nusselt number, friction factor, and thermal performance factor are discussed.

#### 4.1 Temperature field

The temperature distributions of various studied cases at four different axial locations (0.6 m, 0.652 m, 0.715 m and 0.793 m) for  $Re = 12000$  are depicted in Fig. 6. As can be seen, for the plain double pipe heat exchanger (P-DPHE) in different locations, the temperature distributions are almost

the same. Moreover, the fluid flow with lower temperature is located near the tube wall and by moving towards tube center, fluid flow with higher temperature is observable. For other cases in which there exist insertion of twisted tape into the inner tube side, due to the generated swirling flow, fluid with lower temperature gradually moves from tube wall towards tube center. As a result, fluid mixing is done well. For the typical twisted tape (TT), it can be said that the temperature distribution is divided into two sections on both sides of the tape. By moving along flow path, the high-temperature fluid forms a half-circle distribution in each section, for which diameter decreases gradually. These changes are identical on both sides of the tape.

**Fig. 5** Comparison of obtained results from numerical simulations (with different turbulence model) with empirical correlations for (a-b) P-DPHE and (c-d) DPHE with TT

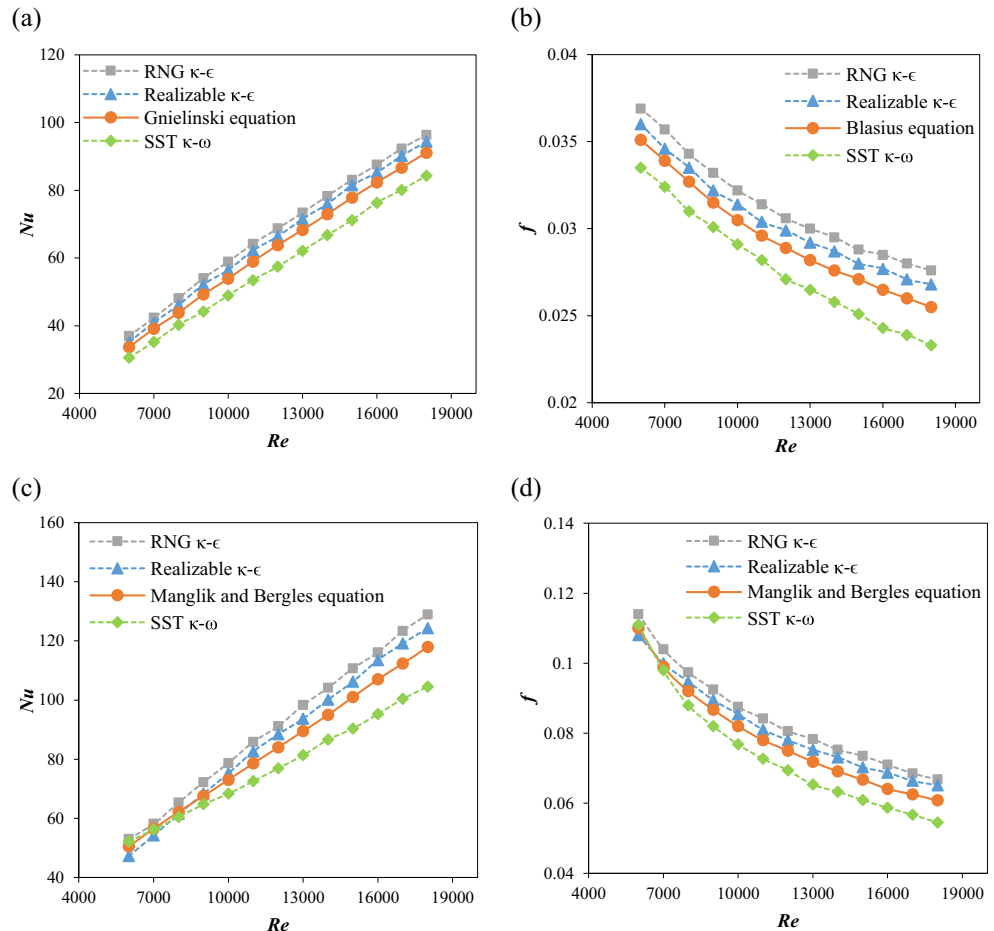
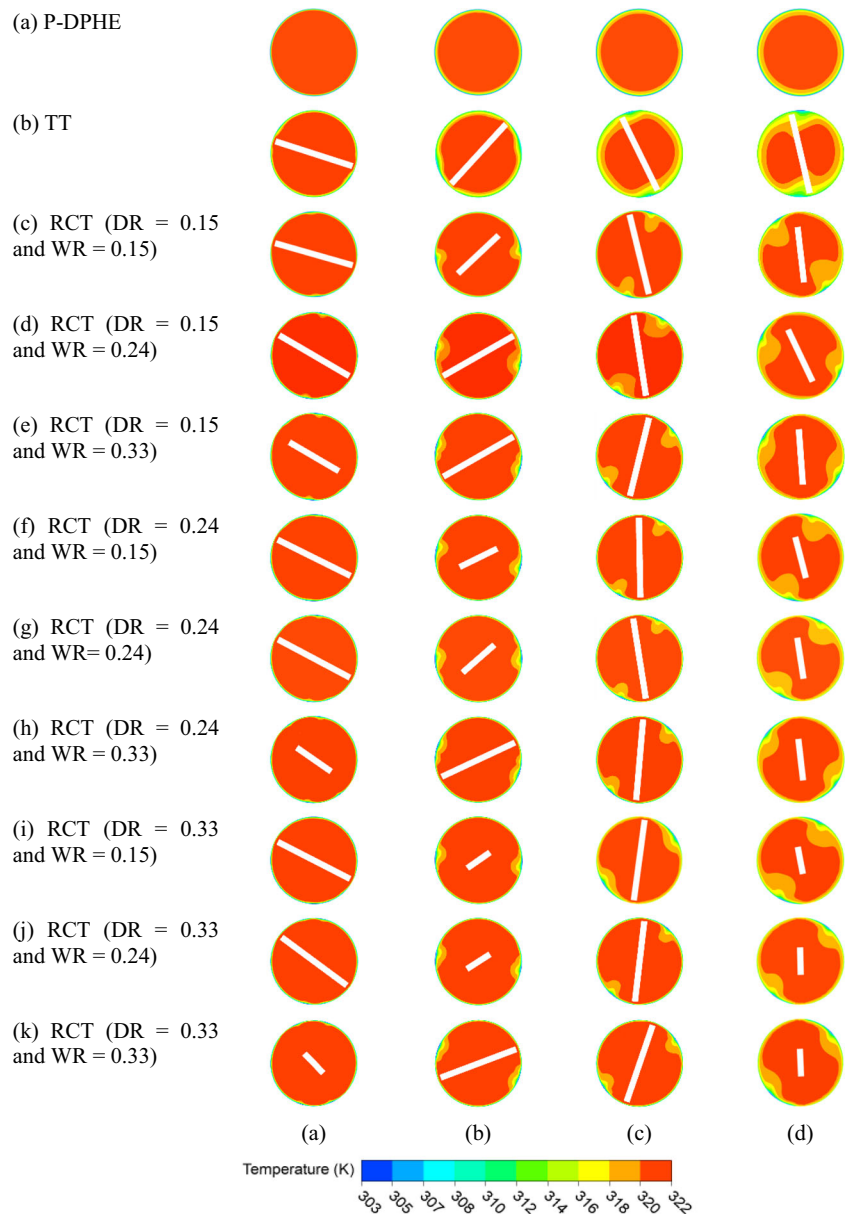




**Fig. 6** Contour plot of temperature for (a) P-DPHE, (b) DPHE with TT and (c-k) DPHE with RCT at axial location (a) 0.6 m, (b) 0.652 m, (c) 0.715 m and (d) 0.793 m for  $Re = 12,000$



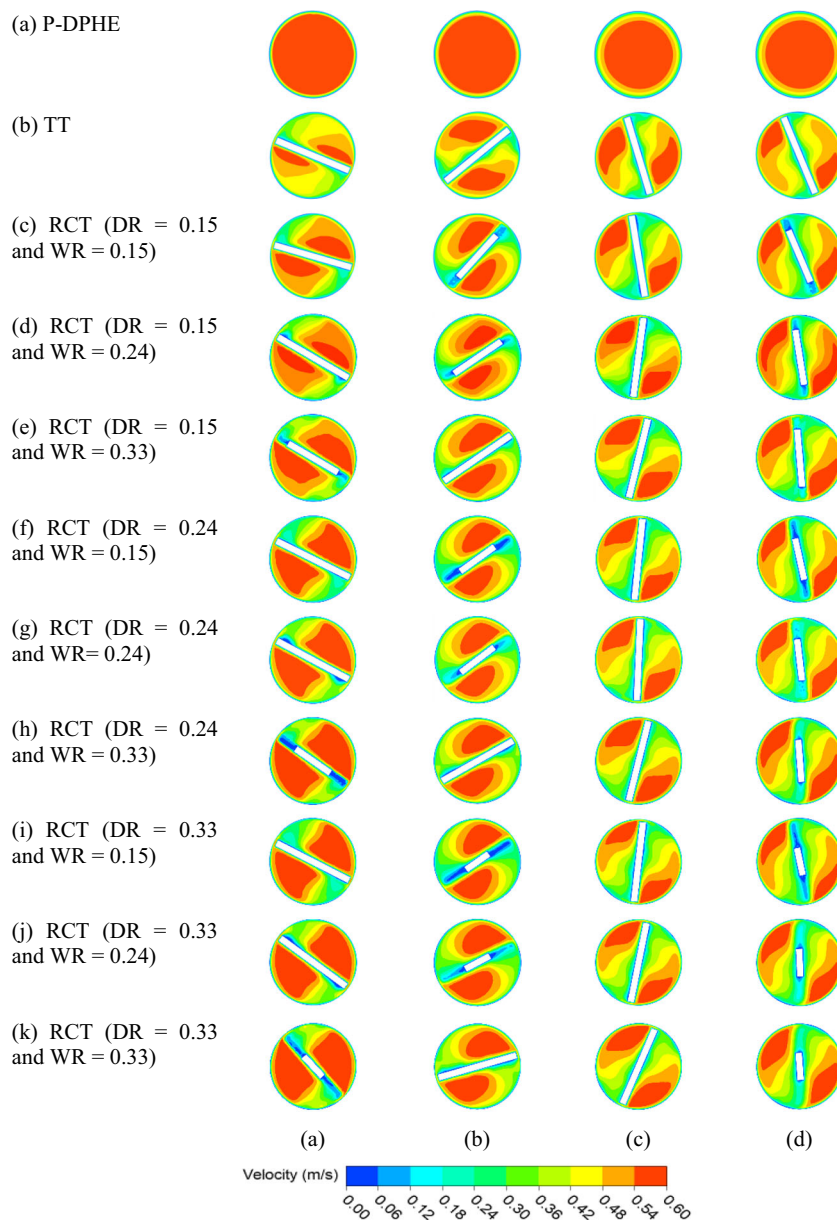
However, for the rectangular cut twisted tapes (RCTs), due to the presence of cuts on the tape edges, the fluid flows with the higher temperature on both sides of the tape are combined with each other and form a S-shaped distribution. Moreover, by moving along the flow direction, the fluid flow with lower temperature draw toward the center of the tape, symmetrically.

#### 4.2 Velocity distributions and vectors

The Fig. 7 shows the tangential velocity distribution field for different cases. Similar to the temperature distribution, the empty inner tube of double pipe heat exchanger preserve approximately the same conditions along the flow direction. This means that fluid velocity reaches its maximum value in

the center of the tube and by approaching the tube wall, fluid velocity reduces. For typically twisted tapes and rectangular cut twisted tapes, the velocity distribution is almost the same in which the higher velocity of the fluid is symmetrically located on both sides of the tapes and by moving along the fluid flow, the maximum velocity area becomes smaller and extends to the vicinity of the tube wall. Figure 8 shows the velocity vector in cross-sectional planes for the empty tube, and the tube fitted with TT/RCT. As can be seen, a common axial flow was found for the plain tube, but it is converted to the swirling flow due to the existence of the insert inside the tube. For the RCT, several vortexes are formed near the cuts, which increases turbulence intensity. This phenomenon results in better mixing of flow. This leads to more heat transfer rate between hot and cold water.

**Fig. 7** Contour plot of velocity for (a) P-DPHE, (b) DPHE with TT and (c-k) DPHE with RCT at axial location (a) 0.6 m, (b) 0.652 m, (c) 0.715 m and (d) 0.793 m for  $Re = 12,000$



### 4.3 Turbulence kinetic energy

The effect of the different cases on the turbulent kinetic energy (TKE) distribution along the fluid flow is demonstrated in Fig. 9. As it is mentioned above, for the empty tube fluid flow around the tube wall has lower velocity, which results in higher kinetic energy occurring in these regions and also relatively constant trend along the flow direction. For a typical twisted tape, by moving along the fluid flow, the TKE gradually increases around the tapes. In the case of using rectangular cut twisted tapes, the higher turbulent kinetic energy occurs near the cutting regions, which indicates the reinforce of flow turbulent intensity and is more significant by increasing the cut depth ratios (it is more

visible on the last plane section). Moreover, in Fig. 10, the TKE distribution for the rectangular cut twisted tape is shown, which indicates that higher turbulent kinetic energy has occurred on its cut edges. By moving toward the tape center, this value decreases.

### 4.4 Heat transfer

The result of the thermal study that has been carried out for various cases is shown in Fig. 11a. This figure demonstrates the relationship between heat transfer rate ( $Nu$ ) and Reynolds number for different simulations including: plain double pipe heat exchanger (P-DPHE), double pipe heat exchanger fitted with typical twisted tape (TT) or rectangular cut twisted tapes (RCT) at

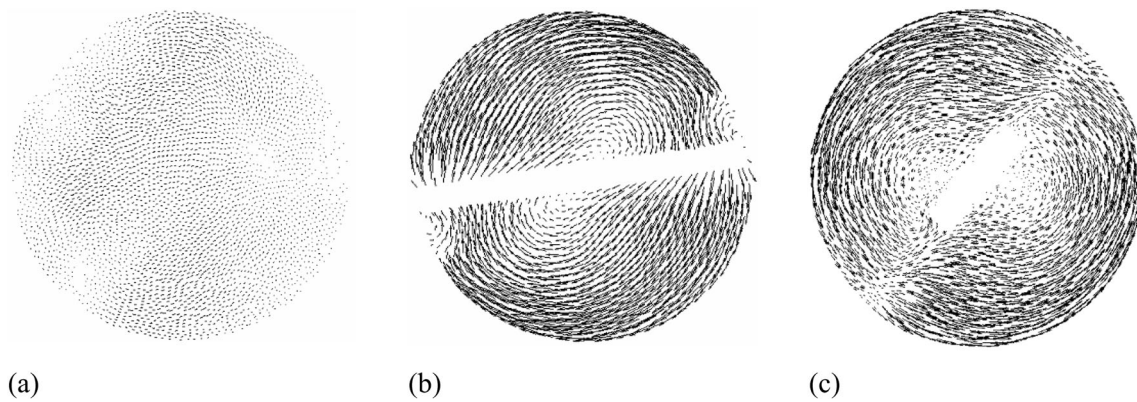


**Fig. 8** Velocity vector diagrams in cross-sectional planes for (a) P-DPHE (b) DPHE with TT (c) and DPHE with RCT

different depth ratios ( $DR = d/W = 0.15, 0.24$  and  $0.33$ ) and width ratios ( $WR = w/W = 0.15, 0.24$  and  $0.33$ ). As can be seen, by increasing the Reynolds number, the Nusselt number increases in all the states. Moreover, by insertion of the twisted tapes, due to the increase of the fluid turbulence, the Nusselt number is increased in comparison with the P-DPHE. In the meanwhile, by using RCTs this increase is higher in comparison with the cases of TT usage. The first reason is the formation of additional disturbance around the rectangular cuts [5, 29, 30, 33]. The other reason is the swirling flow, which causes a better mix of the fluid in the center with the fluid around the tube wall. This phenomenon makes the hot fluid to be more in contact with the common wall between the hot and cold water. These factors increase the radial and tangential velocity of the fluid and make the boundary layer thinner [11, 28] which will cause a rise in heat transfer rate. Furthermore, it could be determined from Fig. 11a that for RCTs at constant Reynolds number, by increasing depth ratio and decreasing width ratio, the Nusselt number increases which are due to increased severity of vortices formed near cuts. The highest rise is related to the  $DR = 0.33$  and  $WR = 0.15$  state and the least increase is related to the  $DR = 0.15$  and  $WR = 0.33$  case which is 175%–192% and 75%–89% higher than the P-DPHE and 105%–118% and 32%–43% higher than DPHE with TT, respectively. From Fig. 11b it was apparent that with increasing Reynolds number, the Nusselt number ratio ( $Nu/Nu_p$ ) tended to decrease. Since in lower Reynolds number due to the thickness of the thermal boundary layer, the influence of RCT insert is more dominant on the destruction of the thermal/velocity boundary layer [11, 14, 27]. Moreover, the  $Nu/Nu_p$  ratio for all cases is higher than unity which represents a beneficial gain for heat transfer enhancement by using the RCTs inserts over the P-DPHE.

#### 4.5 Friction factor

The hydraulic study has been carried out for different cases depicted in Fig. 12a–b. The variations of friction factor versus the Reynolds number for the double pipe heat exchanger with/without TT and also double pipe heat exchanger with RCTs at different rectangular cut depth ratios ( $DR = d/W = 0.15, 0.24, 0.33$ ) and width ratios ( $WR = w/W = 0.15, 0.24, 0.33$ ) is obvious (Fig. 12a). It is seen that in all the cases the friction factor continues to decrease with increasing Reynolds number. In the cases that the heat exchanger is equipped with twisted tapes, the friction factor is higher than that for the P-DPHE.

Using RCTs, flow turbulence increases. The reason is reduction of flow areas. Moreover, the secondary flow comes in more tangential contact with the common wall and this will result in fluctuation and vortex formation. As a result, the friction factor increases in comparison with the heat exchanger with TT. It should be noted that the pressure drop due to the blocking of the flow increases, as well. By investigating the graph, it is determined that by increasing DR and decreasing WR the friction factor increases for RCTs, which is similar to the results mentioned for the Nusselt number. This is due to the termination of boundary layer development close to the inner tube wall during the course of flow [35]. The increase in friction factor by using RCT is found to be in the range of 5.02–8.84 and 1.79–3.43 times, over those of the corresponding DPHE with/without TT respectively. The highest increase is related to the case of  $DR = 0.33$  and  $WR = 0.15$  and the least increase is related to the case of  $DR = 0.15$  and  $WR = 0.33$ . The variation of  $f/f_p$  against Re as shown in Fig. 12b. As can be seen, with increasing Reynolds number the  $f/f_p$  increases with a slight slope.

#### 4.6 Thermal performance factor

Thermal performance factor is one of the parameters which is essential for determining the thermal-hydraulic performance

**Fig. 9** Contour plot of turbulent kinetic energy (TKE) for (a) P-DPHE, (b) DPHE with TT and (c-k) DPHE with RCT at axial location (a) 0.6 m, (b) 0.652 m, (c) 0.715 m and (d) 0.793 m for  $Re = 12,000$

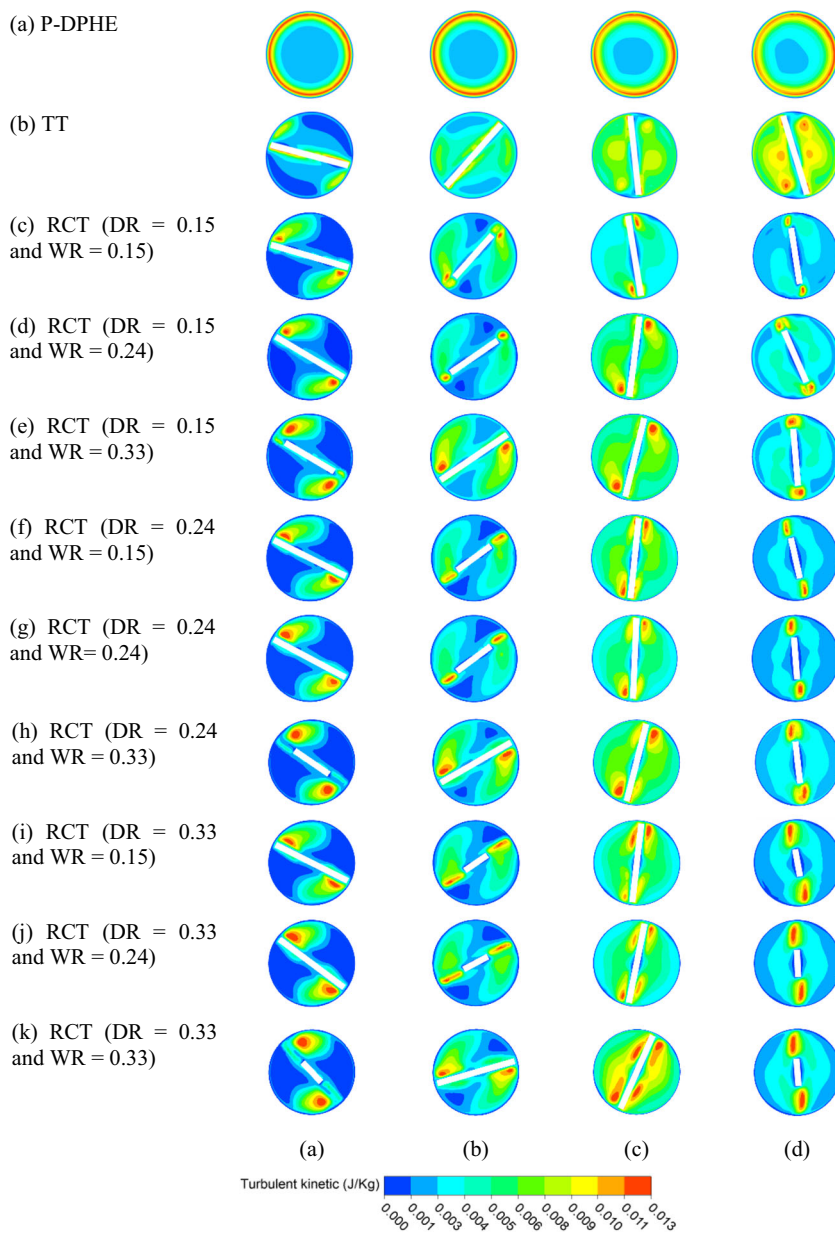


**Fig. 10** TKE distributions for rectangular cut twisted tape

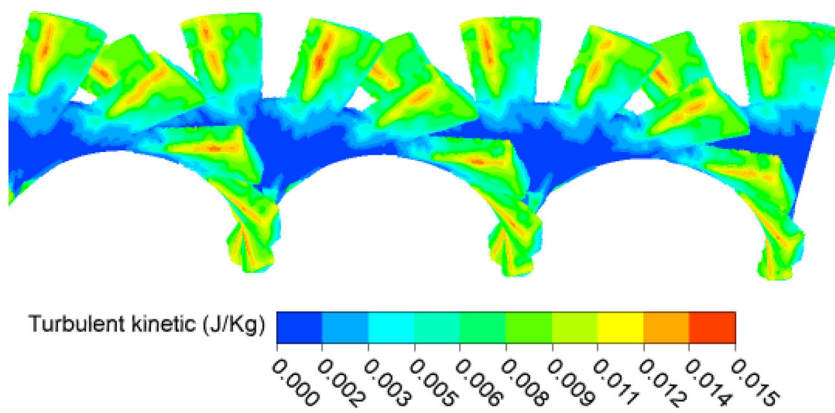
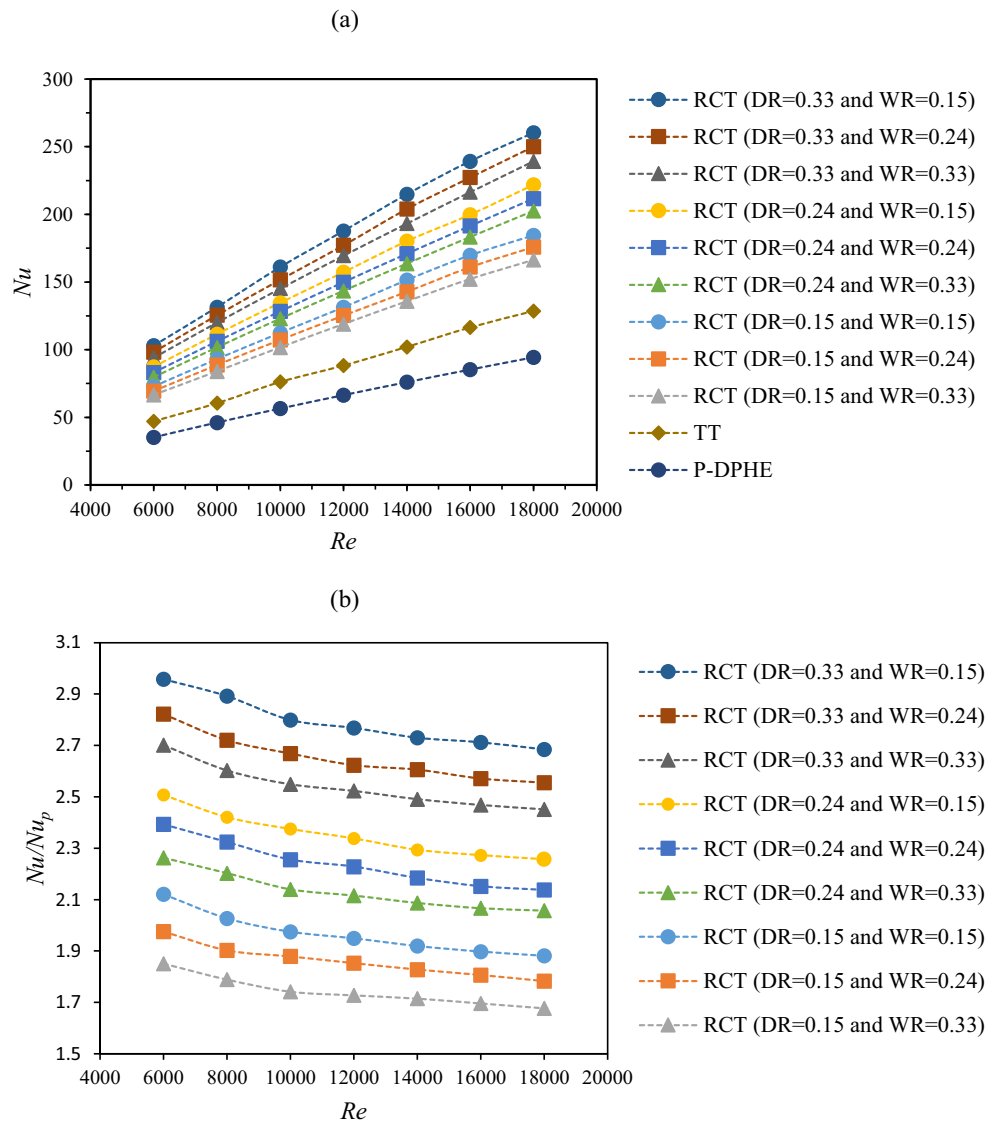


**Fig. 11** Effect of rectangular cut depth ratios (DR) and rectangular cut width ratios (WR) on (a)  $Nu$  and (b)  $Nu/Nu_p$



of a heat exchanger. In a constant pumping power, the thermal-hydraulic performance of identical tubes with and without twisted were investigated by making use of eq. (28).

$$TPF = \frac{Nu}{Nu_p} \left( \frac{f}{f_p} \right)^{-1/3} \tag{28}$$

Where  $Nu_p$  and  $f_p$  correspond to plain tube and  $Nu$  and  $f$  are related to the tube equipped with twisted tape.

Variation of the thermal performance factor versus the Reynolds number for double pipe heat exchanger with TT/RCT is shown in Fig. 13. In general, it is seen that for all the cases the thermal performance factor tends to decrease with increasing the Reynolds number. For RCTs, the thermal performance factor at constant pumping power is higher than TT for all rectangular cut depth ratios (DR) and width ratios (WR) which is

principally influenced by a lower friction loss penalty. The results also reveal that by increasing the DR and WR, the TPF increases and decreases respectively. The reason for this phenomenon can be attributed to the generation of stronger turbulence which results in increased heat transfer rate. The highest increase is related to the case of DR = 0.33 and WR = 0.15 and the least increase is related to the case of DR = 0.15 and WR = 0.33 that varies from 39.7% to 43% and 6.1% to 8.5% respectively, in comparison with TT. The three-dimensional plot for rectangular cut twisted tape in terms of depth ratio and width ratio is exhibited in Fig. 14. It is specified that the maximum thermal performance factor is about 1.46 that achieved for DR = 0.33 and WR = 0.15 and represents the optimal condition from energy saving point of view in the present study.

**Fig. 12** Effect of rectangular cut depth ratios (DR) and rectangular cut width ratios (WR) on (a)  $f$  and (b)  $f/f_p$

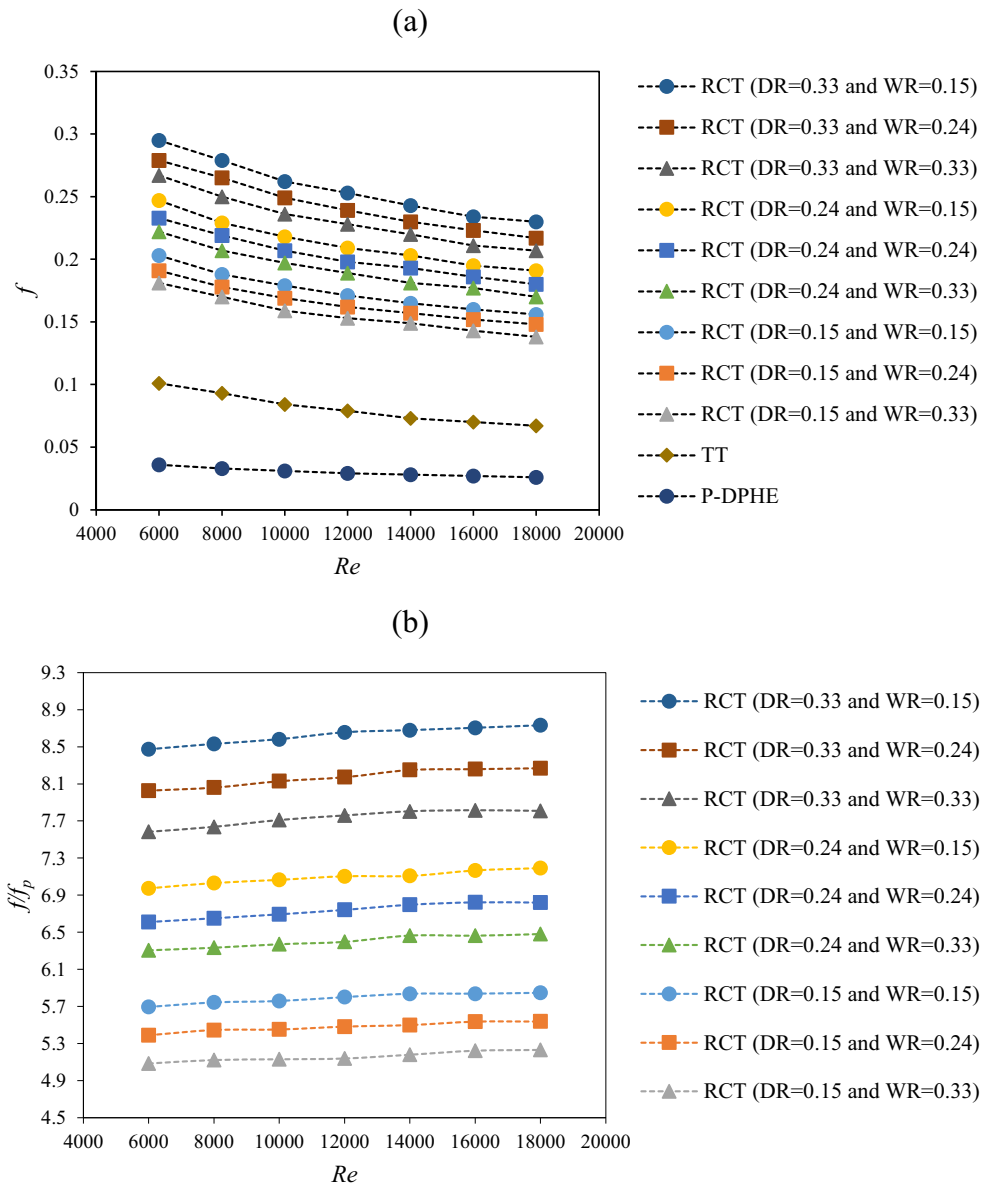
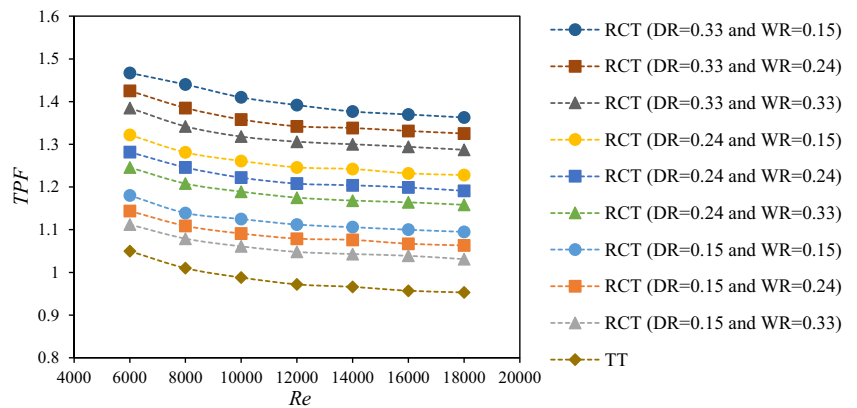


**Fig. 13** Effect of rectangular cut depth ratio (DR) and rectangular cut width ratio (WR) on TPF



#### 4.7 New correlations development

In this study, regression analysis was employed to find out the correlations between different variables based on the numerical results. These variables are: cut depth ratio ( $d/W$ ), cut width ratio ( $w/W$ ), Reynolds number, Prandtl number, Nusselt number and friction factor. The correlations are of the form:

$$Nu = 0.0153Re^{0.85}Pr^{0.78} \left(1 + \left(\frac{d}{W}\right)\right)^{2.38} \left(1 + \left(\frac{w}{W}\right)\right)^{-0.63} \quad (29)$$

$$f = 1.075Re^{-0.23} \left(1 + \left(\frac{d}{W}\right)\right)^{2.64} \left(1 + \left(\frac{w}{W}\right)\right)^{-0.68} \quad (30)$$

For Eq. (29) and Eq. (30) the R-square value is 0.9874 and 0.9861 respectively, which means that the fit explains 98.74% and 98.61% of the total variation in the data about the average. The fit standard error of the random component in the numerical data is about 3%.

#### 5 Comparison of results with previous studies

Different studies have been carried out for investigating the influence of modified twisted tapes insertion in a tube on the heat transfer rate and thermal performance factor. Some of these tapes are illustrated in Fig. 15 for which the performance is compared with the optimal case of the present study (rectangular cut twisted tape with  $DR = 0.33$  and  $WR = 0.15$ ) in Fig. 16. These modified twisted tapes are: twin counter twisted tapes [25], alternate-axis triangular cut twisted tape [15], twisted tape with center wings and alternate-axes [26], twisted tape with uniform alternate length [27], alternate clock-wise

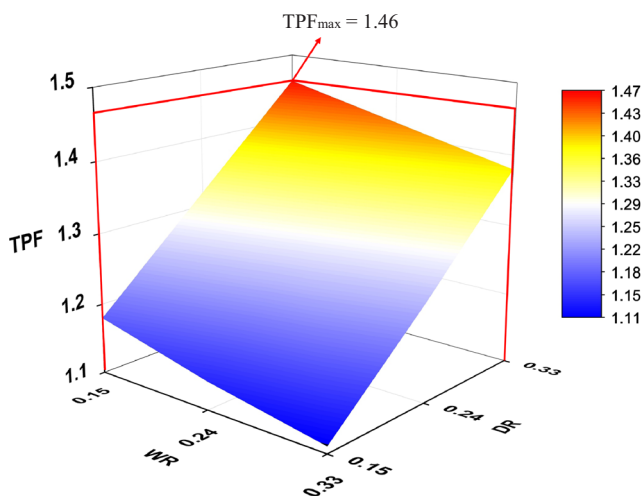


**Fig. 14** 3D plot for variation of TPF versus rectangular cut depth ratios (DR) and width ratios (WR) at  $Re = 6000$

and counterclockwise twisted tapes [28], perforated twisted tapes with parallel wings [20], perforated helical twisted-tapes [14], peripherally-cut twisted tape [29], oblique delta-winglet twisted tape [30], perforated twisted tapes [19], peripherally-cut twisted tape with alternate axis [34]. According to Fig. 16, the rectangular cut twisted tape has a better performance than the other modified tapes.

#### 6 Conclusions

In this article, a double pipe heat exchanger (DPHE) with a rectangular cut twisted tape (RCT) in its inner tube side was investigated. Different cut depth ratios ( $DR = d/W = 0.15, 0.24$  and  $0.33$ ) and cut width ratios ( $WR = w/W = 0.15, 0.24$  and  $0.33$ ) for constant twist ratio ( $Y = 3.0$ ) were considered during the numerical study. The achieved results were compared with plain double pipe heat exchanger (P-DPHE) and double pipe heat exchanger fitted with typical twisted tape (TT). The results of the study have been reported in the form of heat transfer (Nu), friction factor (f) and thermal performance factor (TPF). Moreover, the temperature, velocity, and turbulent kinetic energy (TKE) contour plots are provided. The Reynolds number range was between 6000 and 18,000. The realizable  $\kappa$ - $\epsilon$  turbulence model was used to simulate the flow. The summary of obtained numerical results is as follows:

- 1) In all the cases that RCTs are used, due to the increases of flow turbulence intensity, the heat transfer rate (Nu) is higher than heat exchanger with/without TT. By increasing cut depth ratios and decreasing cut width ratios, the heat transfer rate shows an increasing trend. For the RCTs the Nusselt number increases in the range of 75% to 192% and 32% to 118% in comparison with TT and P-DPHE respectively. The highest increase is related to  $DR = 0.33$  and  $WR = 0.15$  and the least increase is related to  $DR = 0.15$  and  $WR = 0.33$ .
- 2) The RCTs provide higher turbulence and vorticity near rectangular cuts region. Moreover, due to increasing fluid tangential contact with the inner tube wall, they have a higher friction factor in comparison with the DPHE with/without TT. This increase is directly and inversely proportional to DR and WR respectively. The higher friction factor was obtained for the case of  $DR = 0.33$  and  $WR = 0.15$  and the lower friction factor resulted for the case of  $DR = 0.15$  and  $WR = 0.33$ . The RCTs friction factor is 5.02 to 8.84 and 1.79 to 3.43 times higher than heat exchanger with/without TT respectively.
- 3) The thermal performance factor of the double pipe heat exchanger with twisted tapes (TT or RCT) shows a decreasing trend with the increase of Reynolds number. For the RCTs with increasing cut depth ratios and width

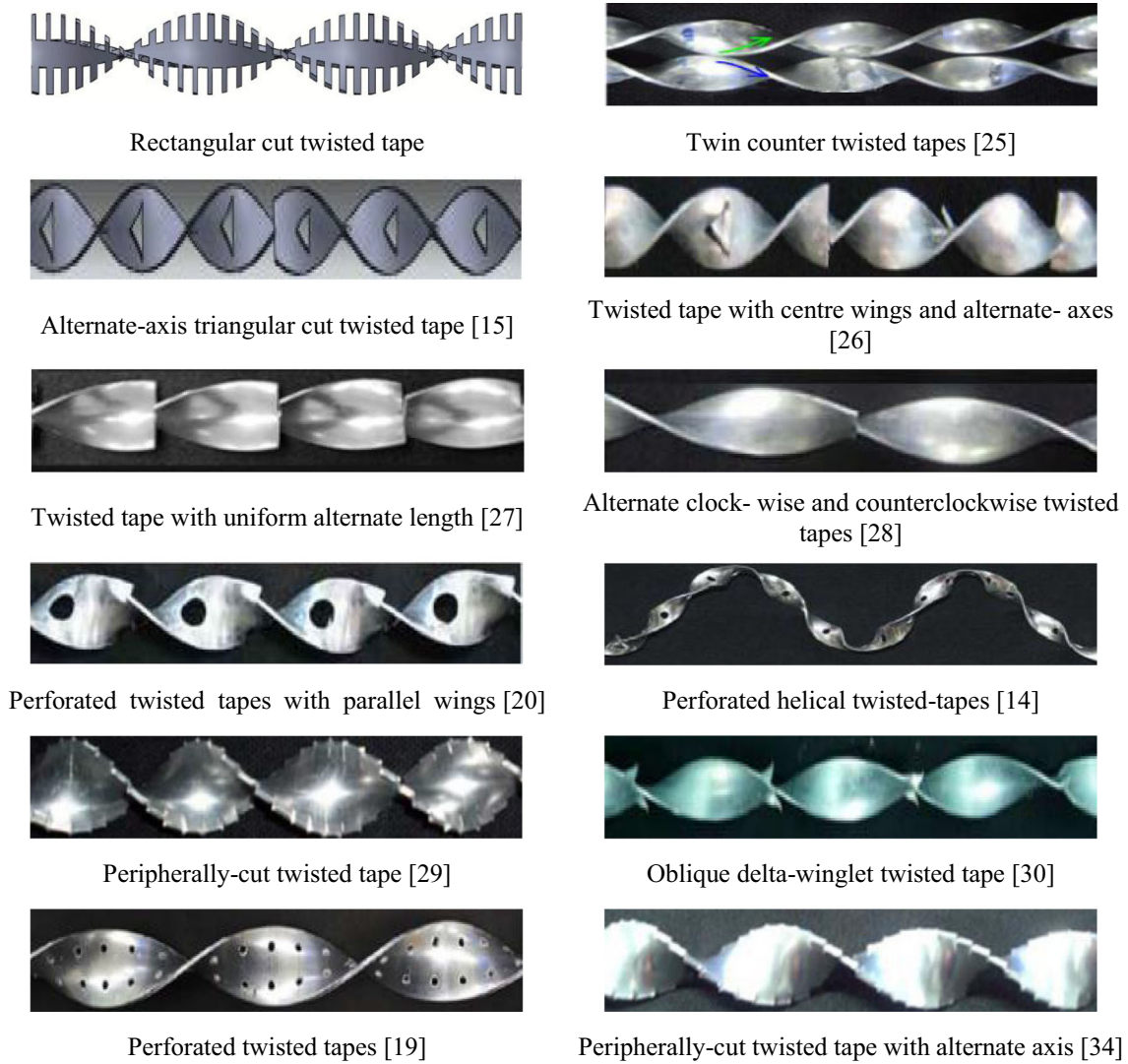
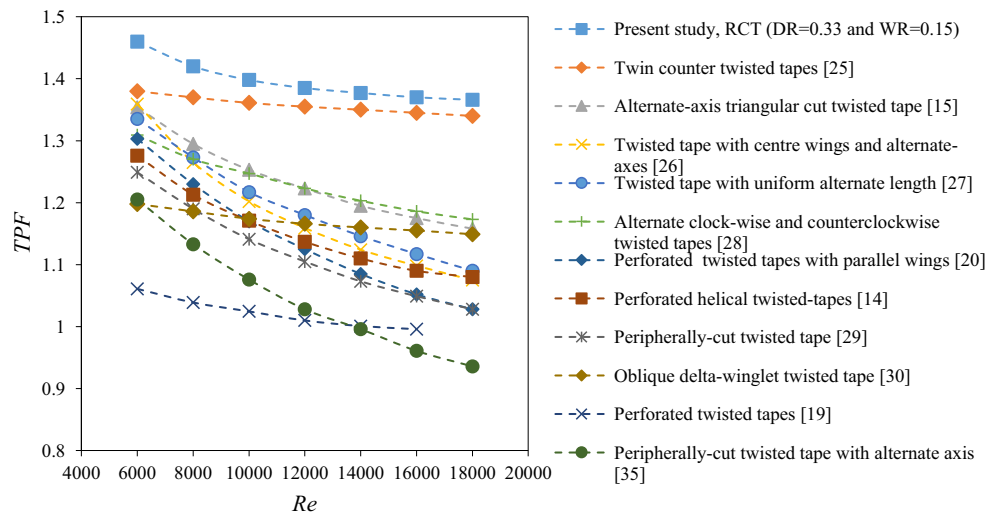


Fig. 15 Selected modified twisted tapes from previous study to compared with present study optimal case

Fig. 16 Comparison between performance of optimum case in present study and previously used modified twisted tapes





ratios, the thermal performance factor increases and decreases respectively. However, it is always higher than the thermal performance factor for typical twisted tape. This highest TPF is about 1.46 that is obtained at lower Reynolds number ( $Re = 6000$ ) for  $DR = 0.33$  and  $WR = 0.15$ .

- 4) For the RCTs, new correlations were developed as a function of rectangular cut depth ratio ( $DR$ ) and width ratio ( $WR$ ) by using regression model in order to estimate the Nusselt number and the friction factor.
- 5) The main advantage of using RCTs in heat exchangers is the significant increase of heat transfer rate. Therefore, they can be used in power stations, air conditions, chemical plants, etc. to have higher heat transfer rate and thermal performance factor.

### Compliance with ethical standards

**Conflict of interest** On behalf of all authors, the corresponding author states that there is no conflict of interest.

### References

1. Liu S, Sakr M (2013) A comprehensive review on passive heat transfer enhancements in pipe exchangers. *Renew Sust Energ Rev* 19:64–81
2. Azimi SS, Kalbasi M (2014) Numerical study of dynamic thermal conductivity of nanofluid in the forced convective heat transfer. *Appl Math Model* 38:1373–1384
3. Bas H, Ozceyhan V (2012) Heat transfer enhancement in a tube with twisted tape inserts placed separately from the tube wall. *Exp Thermal Fluid Sci* 41:51–58
4. Bhuiya M, Chowdhury M, Shahabuddin M, Saha M, Memon L (2013) Thermal characteristics in a heat exchanger tube fitted with triple twisted tape inserts. *International Communications in Heat and Mass Transfer* 48:124–132
5. Hasanpour A, Farhadi M, Sedighi K (2016) Experimental heat transfer and pressure drop study on typical, perforated, V-cut and U-cut twisted tapes in a helically corrugated heat exchanger. *International Communications in Heat and Mass Transfer* 71:126–136
6. Piriyaunrod N, Eiamsa-Ard S, Thianpong C, Pimsarn M, Nanan K (2015) Heat transfer enhancement by tapered twisted tape inserts. *Chem Eng Process Process Intensif* 96:62–71
7. Rahimi M, Shabaniyan SR, Alsairafi AA (2009) Experimental and CFD studies on heat transfer and friction factor characteristics of a tube equipped with modified twisted tape inserts. *Chem Eng Process Process Intensif* 48:762–770
8. Rehman MU, Siddique W, Haq I, Ali N, Farooqi Z (2016) CFD analysis of the influence of guide ribs/vanes on the heat transfer enhancement of a trapezoidal channel. *Appl Therm Eng* 102:570–585
9. Tamna S, Kaewkohkiat Y, Skullong S, Promvong P (2016) Heat transfer enhancement in tubular heat exchanger with double V-ribbed twisted-tapes. *Case studies in thermal engineering* 7:14–24
10. Zhang X, Liu Z, Liu W (2012) Numerical studies on heat transfer and flow characteristics for laminar flow in a tube with multiple regularly spaced twisted tapes. *Int J Therm Sci* 58:157–167
11. Skullong S, Promvong P, Thianpong C, Jayranaiwachira N, Pimsarn M (2018) Thermal performance of heat exchanger tube inserted with curved-winglet tapes. *Appl Therm Eng* 129:1197–1211
12. Zhang X, Liu Z, Liu W (2013) Numerical studies on heat transfer and friction factor characteristics of a tube fitted with helical screw-tape without core-rod inserts. *Int J Heat Mass Transf* 60:490–498
13. He Y, Liu L, Li P, Ma L (2018) Experimental study on heat transfer enhancement characteristics of tube with cross hollow twisted tape inserts. *Appl Therm Eng* 131:743–749
14. Nanan K, Thianpong C, Promvong P, Eiamsa-Ard S (2014) Investigation of heat transfer enhancement by perforated helical twisted-tapes. *International Communications in Heat and Mass Transfer* 52:106–112
15. Oni TO, Paul MC (2016) Numerical investigation of heat transfer and fluid flow of water through a circular tube induced with divers' tape inserts. *Appl Therm Eng* 98:157–168
16. Mashoofi N, Pourahmad S, Pesteei S (2017) Study the effect of axially perforated twisted tapes on the thermal performance enhancement factor of a double tube heat exchanger. *Case studies in thermal engineering* 10:161–168
17. Sroysroy A, Eiamsa-ard S (2017) Periodically fully-developed heat and fluid flow behaviors in a turbulent tube flow with square-cut twisted tape inserts. *Appl Therm Eng* 112:895–910
18. Suri ARS, Kumar A, Maithani R (2017) Heat transfer enhancement of heat exchanger tube with multiple square perforated twisted tape inserts: experimental investigation and correlation development. *Chem Eng Process Process Intensif* 116:76–96
19. Thianpong C, Eiamsa-Ard P, Eiamsa-Ard S (2012) Heat transfer and thermal performance characteristics of heat exchanger tube fitted with perforated twisted-tapes. *Heat Mass Transf* 48:881–892
20. Thianpong C, Eiamsa-Ard P, Promvong P, Eiamsa-Ard S (2012) Effect of perforated twisted-tapes with parallel wings on heat transfer enhancement in a heat exchanger tube. *Energy Procedia* 14:1117–1123
21. Man C, Lv X, Hu J, Sun P, Tang Y (2017) Experimental study on effect of heat transfer enhancement for single-phase forced convective flow with twisted tape inserts. *Int J Heat Mass Transf* 106:877–883
22. Ferroni P, Block R, Todreas N, Bergles A (2011) Experimental evaluation of pressure drop in round tubes provided with physically separated, multiple, short-length twisted tapes. *Exp Thermal Fluid Sci* 35:1357–1369
23. Eiamsa-ard S, Thianpong C, Promvong P (2006) Experimental investigation of heat transfer and flow friction in a circular tube fitted with regularly spaced twisted tape elements. *International Communications in Heat and Mass Transfer* 33:1225–1233
24. Zheng L, Xie Y, Zhang D (2017) Numerical investigation on heat transfer performance and flow characteristics in circular tubes with dimpled twisted tapes using  $Al_2O_3$ -water nanofluid. *Int J Heat Mass Transf* 111:962–981
25. Eiamsa-Ard S, Thianpong C, Eiamsa-Ard P (2010) Turbulent heat transfer enhancement by counter/co-swirling flow in a tube fitted with twin twisted tapes. *Exp Thermal Fluid Sci* 34:53–62
26. Eiamsa-Ard S, Wongcharee K, Eiamsa-Ard P, Thianpong C (2010) Thermohydraulic investigation of turbulent flow through a round tube equipped with twisted tapes consisting of centre wings and alternate-axes. *Exp Thermal Fluid Sci* 34:1151–1161
27. Eiamsa-ard S, Somkleang P, Nuntadusit C, Thianpong C (2013) Heat transfer enhancement in tube by inserting uniform/non-uniform twisted-tapes with alternate axes: effect of rotated-axis length. *Appl Therm Eng* 54:289–309
28. Eiamsa-Ard S, Promvong P (2010) Performance assessment in a heat exchanger tube with alternate clockwise and counter-clockwise twisted-tape inserts. *Int J Heat Mass Transf* 53:1364–1372
29. Eiamsa-ard S, Seemawute P, Wongcharee K (2010) Influences of peripherally-cut twisted tape insert on heat transfer and thermal performance characteristics in laminar and turbulent tube flows. *Exp Thermal Fluid Sci* 34:711–719

30. Eiamsa-Ard S, Wongcharee K, Eiamsa-Ard P, Thianpong C (2010) Heat transfer enhancement in a tube using delta-winglet twisted tape inserts. *Appl Therm Eng* 30:310–318
31. El Maakoul A, Laknizi A, Saadeddine S, Abdellah AB, Meziane M, El Metoui M (2017) Numerical design and investigation of heat transfer enhancement and performance for an annulus with continuous helical baffles in a double-pipe heat exchanger. *Energy Convers Manag* 133:76–86
32. Guo J, Xu M, Cheng L (2010) Numerical investigations of circular tube fitted with helical screw-tape inserts from the viewpoint of field synergy principle. *Chem Eng Process Process Intensif* 49: 410–417
33. Murugesan P, Mayilsamy K, Suresh S, Srinivasan P (2011) Heat transfer and pressure drop characteristics in a circular tube fitted with and without V-cut twisted tape insert. *International Communications in Heat and Mass Transfer* 38:329–334
34. Seemawute P, Eiamsa-Ard S (2010) Thermohydraulics of turbulent flow through a round tube by a peripherally-cut twisted tape with an alternate axis. *International Communications in Heat and Mass Transfer* 37:652–659
35. Eiamsa-Ard S, Promvongse P (2010) Thermal characteristics in round tube fitted with serrated twisted tape. *Appl Therm Eng* 30: 1673–1682
36. Murugesan P, Mayilsamy K, Suresh S (2010) Turbulent heat transfer and pressure drop in tube fitted with square-cut twisted tape. *Chin J Chem Eng* 18:609–617
37. Fluent A, "6.3, 2006, *FLUENT 6.3 User's Guide, Fluent, Inc., Lebanon, NH*
38. El Maakoul A, Laknizi A, Saadeddine S, El Metoui M, Zaitte A, Meziane M et al (2016) Numerical comparison of shell-side performance for shell and tube heat exchangers with trefoil-hole, helical and segmental baffles. *Appl Therm Eng* 109:175–185
39. Menter FR (1994) Two-equation eddy-viscosity turbulence models for engineering applications. *AIAA J* 32:1598–1605
40. Kravchenko V (1966) Empirical equation derived of density of heavy water for temperature dependence. *Atomnaya Energiya* 20: 168
41. Azmi W, Sharma K, Sarma P, Mamat R, Anuar S, Sundar LS (2014) Numerical validation of experimental heat transfer coefficient with SiO<sub>2</sub> nanofluid flowing in a tube with twisted tape inserts. *Appl Therm Eng* 73:296–306
42. Gnielinski V (1976) New equations for heat and mass transfer in turbulent pipe and channel flow. *Int Chem Eng* 16:359–368
43. MN Ozisik, *Heat transfer: a basic approach* (1985)
44. Manglik RM, Bergles AE (1993) Heat transfer and pressure drop correlations for twisted-tape inserts in isothermal tubes: Part II—Transition and turbulent flows. *J Heat Transf* 115:890–896

**Publisher's note** Springer Nature remains neutral with regard to jurisdictional claims in published maps and institutional affiliations.